

# A non-equilibrium Monte Carlo approach to potential refinement in inverse problems

Nigel B. Wilding

*Department of Physics, University of Bath, Bath BA2 7AY, United Kingdom*

The inverse problem for a disordered system involves determining the interparticle interaction parameters consistent with a given set of experimental data. Recently, Rutledge has shown (Phys. Rev. **E63**, 021111 (2001)) that such problems can be generally expressed in terms of a grand canonical ensemble of polydisperse particles. Within this framework, one identifies a polydisperse attribute ('pseudo-species')  $\sigma$  corresponding to some appropriate generalized coordinate of the system to hand. Associated with this attribute is a composition distribution  $\bar{\rho}(\sigma)$  measuring the number of particles of each species. Its form is controlled by a conjugate chemical potential distribution  $\mu(\sigma)$  which plays the role of the requisite interparticle interaction potential. Simulation approaches to the inverse problem involve determining the form of  $\mu(\sigma)$  for which  $\bar{\rho}(\sigma)$  matches the available experimental data. The difficulty in doing so is that  $\mu(\sigma)$  is (in general) an unknown *functional* of  $\bar{\rho}(\sigma)$  and must therefore be found by iteration. At high particle densities and for high degrees of polydispersity, strong cross coupling between  $\mu(\sigma)$  and  $\bar{\rho}(\sigma)$  renders this process computationally problematic and laborious. Here we describe an efficient and robust *non-equilibrium* simulation scheme for finding the equilibrium form of  $\mu[\bar{\rho}(\sigma)]$ . The utility of the method is demonstrated by calculating the chemical potential distribution conjugate to a specific log-normal distribution of particle sizes in a polydisperse fluid.

PACS numbers: 61.20Ja, 02.70.Tt

## I. INTRODUCTION AND BACKGROUND

Much of statistical mechanics is concerned with the task of deducing the macroscopic structure of a system, *given* a description of its microscopic interaction interactions. Sometimes, however, one is confronted with the reverse problem: that of determining the form of the interactions from knowledge of the structure. This so-called "inverse problem" [1] arises, for example, when one has scattering measurements of the structure factor of a molecular fluid and wishes to find the corresponding interparticle interaction potentials [2]. Alternatively one might have obtained spectroscopic data for the distribution of orientations of a certain bond in a molecular solid and wish to determine the corresponding bond orientation potential [3].

One approach of longstanding for tackling inverse problems is Reverse Monte Carlo [4]. This simulation scheme seeks to minimize error estimators quantifying the difference between experimentally derived structural data (such as a radial distribution function) and the corresponding simulation averages. The minimization proceeds by replacing the Hamiltonian in the standard MC Metropolis update scheme with the error estimator function, while the role of temperature is replaced by the estimated degree of uncertainty in the experimental data. The method outputs a set of configurations, which are consistent with the experimental data and can be further analyzed, but provides no direct information on the underlying form of the interaction potential, the values of the thermodynamic fields, or fluctuation effects.

Recently, Rutledge [5] has suggested that ostensibly disparate inverse problems can be incorporated within a unifying theoretical framework by mapping them onto a generalized grand canonical polydisperse composition space. The key to achieving this is the identification of

a generalized coordinate of the system,  $\sigma$ , on which the potential function of interest is defined. The problem may then be translated into the language of polydispersity by regarding  $\sigma$  as a continuous variable labeling the species of particles that comprise the system. In general, however, these polydisperse particles need not correspond directly to the real particles of the system, and are perhaps best regarded as 'pseudo particles' the precise identity of which depends on the particular choice of  $\sigma$  and thus on the physical situation to hand. The reformulation is completed by assuming that the number density of pseudo particles of each  $\sigma$  is free to fluctuate. Within the resulting open ensemble, the instantaneous count of particles of each species is measured by a composition distribution  $\rho(\sigma)$ , the ensemble-averaged form of which,  $\bar{\rho}(\sigma)$ , is directly controlled by the conjugate chemical potential distribution  $\mu(\sigma)$  (see Appendix A). The latter quantity plays the role of the potential function of interest.

In practice a surprising variety of inverse problems can be cast in this form. For example, in a liquid crystal, one can identify  $\sigma$  with the orientation of a molecule (cf. [6]) and  $\mu(\sigma)$  with an effective orientational potential. In an atomic crystal,  $\sigma$  can be identified with the phonon frequencies [5] and  $\mu(\sigma)$  to the Fourier transform of the interparticle potential. For a simple monatomic fluid, one can construct a "bond" picture, in which each of the  $N$  real particles is replaced by  $N$  non-interacting pseudo particles, all localized to the site of the real particle. Each pseudo particles is speciated according to its distance to one other nominated real particle and the associated  $\mu(\sigma)$  is simply the interparticle potential [7].

In general, for systems described by two-body particle interactions, a unique relationship is believed to exist between  $\bar{\rho}(\sigma)$  and  $\mu(\sigma)$  [8, 9, 10]. The simulation challenge is then to determine the form of  $\mu(\sigma)$  for which  $\bar{\rho}(\sigma)$

matches some “target” form  $\bar{\rho}_t(\sigma)$  corresponding to the available experimental structural data. The difficulty in achieving this is that  $\mu(\sigma)$  is an unknown *functional* of  $\bar{\rho}(\sigma)$ , and thus must be determined iteratively via some refinement procedure. In the following section we summarize the state-of-the-art in this regard.

## II. ITERATIVE REFINEMENT SCHEMES AND CONVERGENCE ISSUES

Refinement typically commences using some guessed form for the interaction potential  $\mu(\sigma)$ . This serves as input to a Monte Carlo simulation, in the course of which the form of  $\bar{\rho}(\sigma)$  is obtained as a histogram. Once sufficient statistics for  $\bar{\rho}(\sigma)$  have been accumulated, the next and successive iterations modify  $\mu(\sigma)$  to reduce the discrepancy between  $\bar{\rho}(\sigma)$  and the target function  $\rho_t(\sigma)$ . To achieve this Rutledge [5] utilized an iteration scheme based on a zeroth order (i.e. non-interacting or ideal gas) approximation to the chemical potential distribution:

$$\mu^{ig}(\sigma) = \ln(\bar{\rho}(\sigma)) , \quad (1)$$

which can be viewed as the polydisperse generalization of the potential of mean force [11, 12]. Using this approximation to initialize  $\mu(\sigma)$ , the iteration then proceeds according to

$$\mu_{i+1}(\sigma) = \mu_i(\sigma) - \alpha \ln\left(\frac{\bar{\rho}_i(\sigma)}{\rho_t(\sigma)}\right) , \quad (2)$$

where  $\alpha \leq 1$  is a step-size parameter, the value of which must be chosen sufficiently small to ensure that the method converges, but not so small that convergence is excessively slow. Rutledge applied this approach to calculate the effective interparticle interaction potential of a single component fluid consistent with a prescribed radial distribution function. For this particular purpose, his scheme is similar to the potential refinement method of Soper [13].

The efficiency with which inverse problems can be solved is clearly contingent on the convergence rate of the refinement procedure for  $\mu(\sigma)$ . Typically a strategy such as that of Eq. 2 will be effective at low number densities of pseudo particles where the non-interacting approximation retains some degree of accuracy. Difficulties arise, however, at high number densities and for high degrees of polydispersity (ie. slowly varying forms of  $\bar{\rho}(\sigma)$ ). In this regime,  $\mu(\sigma)$  can differ greatly from  $\mu^{ig}(\sigma)$ . Moreover, strong cross coupling between  $\mu(\sigma)$  and  $\bar{\rho}(\sigma)$  implies that variations (within the refinement procedure) to the chemical potential at one value of  $\sigma$  can significantly affect the entire form of  $\bar{\rho}(\sigma)$ . This can seriously impede convergence; the sole remedy being to utilize a small step size  $\alpha$ , with a concomitant increase in the computational effort [14].

In view of these considerations, one might seek to adopt a more sophisticated refinement procedure in the expectation that it will promote faster convergence than Eq. 2. Such schemes have been developed and applied by Lyubartsev & Laaksonen [14] and Tóth [15]. They employ large matrices of derivatives (obtainable via fluctuation relations as ensemble averages) and designed to direct the minimization more reliably in the ‘downhill’ direction in the multidimensional parameter space of some cost function measuring the deviation of  $\bar{\rho}(\sigma)$  from  $\rho_t(\sigma)$ . Whilst in our experience of gradient schemes (we have tried Powell’s method, conjugate gradient methods and variable metric methods [16]), they do provide a more rapid approach towards the solution in the early iterations, we find that they do not converge as reliably (at least for high degrees of polydispersity) as the non-interacting approximation scheme of eq. 2. Instead we have found them to be prone to becoming trapped in local minima of the cost function. Although, empirically, this problem can be ameliorated by mixing iterations [17] of the sophisticated scheme with simple ones of the form Eq. 2, such an *ad-hoc* approach is clearly neither theoretically well-founded nor aesthetically satisfying.

Other recent work, carried out in the context of targeted polydispersity, has examined the utility of histogram extrapolation in targeting a specific composition distribution  $\rho_t(\sigma)$  [18, 19]. Histogram extrapolation [20] allows a histogram for  $\bar{\rho}(\sigma)$  accumulated at some  $\mu(\sigma)$  to be reweighted to provide an estimate for  $\bar{\rho}(\sigma)$  corresponding to some other chemical potential distribution  $\mu'(\sigma)$ . To exploit the method, it can be embedded within a gradient-based scheme to minimize a cost function measuring the deviation of  $\bar{\rho}(\sigma)$  and  $\rho_t(\sigma)$  [19]. In practice, however, one finds that the extrapolation operates effectively only within a limited range of chemical potential space around the simulation state point. If one attempts to extrapolate too far from this point, spurious structure appears in the results and the method may not converge to the correct solution. This problem can be dealt with by constructing a series of intermediate targets that interpolate between the initial guess for  $\bar{\rho}(\sigma)$  and the true target (see ref. [19] for full details).

In addition to the convergence issues already mentioned, a further important matter is the statistical quality of the measured estimate for  $\bar{\rho}_i(\sigma)$ . Unless the ‘signal-to-noise’ ratio associated with this measurement is sufficiently high prior to each iteration, the procedure will necessarily fail to converge. Often, however, one has no ready criteria for knowing when the statistical quality of the data is “good enough”. We note also in passing that related problems can arise when the statistical quality of the experimentally derived target distribution  $\rho_t(\sigma)$  is poor. Indeed, it has been reported that in such circumstances the solution to which the refinement converges can depend on the initial guess for  $\mu(\sigma)$  [21] or contain spurious features [22]. This would seem to suggest that ‘noise’ in the target can engender additional local minima in the multidimensional parameter space on which

the cost function is defined.

In this paper we describe a new iterative refinement scheme which is simple and straightforward to implement, yet yields a robust and efficient procedure. Our method (which is inspired by, but is distinct from, the flat energy histogram random walk algorithm of Wang and Landau [23]) is based on a non-equilibrium MC procedure in which refinements to  $\mu(\sigma)$  are implemented ‘on-the-fly’ during the simulation, not between iterations as in equilibrium schemes. Empirically we find that the method provides an estimate of the true solution right from the earliest iterations; subsequent iterations merely serve to reduce the statistical uncertainty in this estimate. This attractive feature promotes more reliable convergence than is found in more complicated gradient based schemes. In a comparative test, the new method is found to be significantly more efficient than the simple equilibrium iteration scheme described by eq. 2.

### III. NON-EQUILIBRIUM REFINEMENT SCHEME

We consider systems having a polydisperse attribute  $\sigma$  varying continuously in the range  $0 \leq \sigma \leq \sigma_c$ . The associated composition distribution  $\rho(\sigma)$  (defined in appendix A) and its conjugate chemical potential distribution are represented as histograms formed by binning the  $\sigma$ -domain into an integer number  $M$  of sub-intervals. A discussion of this binning strategy can be found in ref. [19].

Given some prescribed target histogram  $\rho_t(\sigma)$ , the refinement  $\mu(\sigma)$  proceeds iteratively using MC simulation. In general, no special bootstrapping measures are necessary for initializing  $\mu(\sigma)$  and, in the absence of a better guess, one can simply take  $\mu(\sigma) = C \forall \sigma$ , with  $C$  an arbitrary constant. During the course of an iteration, the chemical potential distribution is modified at regular short intervals (eg. every 10 MC sweeps). The modification continuously tunes  $\mu(\sigma)$  such as to minimize the deviation of the *instantaneous* composition distribution  $\rho(\sigma)$  from its target value:

$$\mu'(\sigma) = \mu(\sigma) - \beta_i \left( \frac{\rho(\sigma) - \rho_t(\sigma)}{\rho_t(\sigma)} \right) \quad \forall \sigma, \quad (3)$$

where  $\beta_i$  is the modification factor for the  $i$ th iteration. Updating  $\mu(\sigma)$  ‘on-the-fly’ in this manner quickly reduces differences between  $\rho(\sigma)$  and its target [24].

The criterion by which an iteration is deemed to have completed is based on the maximum value, across the range of  $\sigma$ , of the relative deviation of the *average* composition distribution from the target form:

$$\zeta = \max \left( \left| \frac{\bar{\rho}_i(\sigma) - \rho_t(\sigma)}{\rho_t(\sigma)} \right| \right). \quad (4)$$

Once  $\zeta$  falls below some previously specified threshold value  $\zeta^*$ ,  $\mu(\sigma)$  can be saved and used as the starting point for the second iteration. This proceeds similarly to the first iteration, except that the value of the modification factor  $\beta$  is reduced, viz

$$\beta_{i+1} = \beta_i/n, \quad (5)$$

with  $n$  some (small) integer [25].

Successive further iterations steadily reduce  $\beta$  towards zero, thereby restoring detailed balance and driving  $\mu(\sigma)$  towards its equilibrium limiting form. For sufficiently large  $i$  (i.e. sufficiently small  $\beta_i$ ),  $\mu_i(\sigma)$  provides a good approximation to this limiting form. If desired, however, one can extrapolate fully to the equilibrium limit by performing a final run with  $\beta = 0$ , followed by application of histogram extrapolation [19, 20] to  $\mu(\sigma)$  in order to match  $\bar{\rho}(\sigma)$  to  $\rho_t(\sigma)$ .

### IV. RESULTS

In order to gauge the efficacy of our scheme we have tested it on a challenging problem: namely that of determining the chemical potential distribution for a fluid of polydisperse Lennard-Jones (LJ) particles having an extremely broad distribution of sizes.

The interparticle potential between two particles labeled  $i$  and  $j$  is given by

$$u(r_{ij}) = 4\epsilon_{ij} \left[ \left( \frac{\sigma_{ij}}{r_{ij}} \right)^{12} - \left( \frac{\sigma_{ij}}{r_{ij}} \right)^6 \right], \quad (6)$$

with  $\sigma_{ij}$  given by the additive mixing rule

$$\sigma_{ij} = (\sigma_i + \sigma_j)/2. \quad (7)$$

The target distribution of particle diameters  $\sigma$  appearing in eq. 7 was assigned a log-normal form, described by the normalized shape function:

$$f(\sigma) = \frac{1 + W^2}{\bar{\sigma} \sqrt{2\pi \ln(1 + W^2)}} \times \exp \left( - \frac{[\ln(\sigma/\bar{\sigma}) + (3/2) \ln(1 + W^2)]^2}{2 \ln(1 + W^2)} \right). \quad (8)$$

Here  $\bar{\sigma}$  is the average particle diameter and  $W$  is the standard deviation in units of  $\bar{\sigma}$ . The associated target composition distribution follows as  $\rho_t(\sigma) = \rho_t f(\sigma)$ , where  $\rho_t$  is the target number density.

For computational convenience,  $f(\sigma)$  was truncated at  $\sigma_c = 12$ . This choice implies that the largest permitted particle size has a volume 1728 times that of the average particle size ( $\bar{\sigma} = 1$ ). The simulations were performed within a periodic cubic box of side  $L = 90\bar{\sigma}$  and the temperature was set to  $T = 2.35$  (in standard LJ

units [26]). The width and scale of the target polydispersity distribution were set to  $W = 2.5$  and  $\rho_t = 0.0152$  respectively, corresponding to a target volume fraction,  $\eta \approx 13\%$  where

$$\eta \equiv \int_0^{\sigma_c} d\sigma \frac{\pi}{6} \sigma^3 \bar{\rho}(\sigma). \quad (9)$$

Although this volume fraction would not be considered especially high for a pure fluid (the critical volume fraction for a monodisperse LJ fluid is about 16%), it is sufficient in the present context to ensure a high degree of cross coupling between  $\bar{\rho}(\sigma)$  and  $\mu(\sigma)$ .

The grand canonical ensemble Monte Carlo (GCMC) algorithm employed has a Metropolis form [26] and invokes four types of operation: particle displacements, particle insertions, particle deletions and particle resizing; each is attempted with equal frequency. Specific to the polydisperse case is the resizing operation which entails attempting to change the diameter of a nominated particle by an amount drawn from a uniform random deviate constrained to lie in some prescribed range. This range (maximum diameter step-size) is chosen to provide a suitable balance between efficient sampling and a satisfactory acceptance rate at the prevailing number density. As regards the remaining types of moves, these proceed in a manner similar to the monodisperse case [26], except that for insertion attempts the new particle diameter is drawn with uniform probability from the range  $\sigma \in [0, \sigma_c]$ .

Histograms of  $\rho(\sigma)$  and  $\mu(\sigma)$  were formed by partitioning the range  $0 \leq \sigma \leq \sigma_c$  into  $M = 120$  equal intervals. The refinement procedure was initialized by setting  $\mu_0(\sigma) = 0 \forall \sigma$ . The initial modification factor was set to  $\beta_0 = 0.01$  (and halved at each successive iteration), while the threshold value of  $\zeta$  at which an iteration is deemed complete (cf. Eq. 4) was set to  $\zeta^* = 0.4$ . With these parameters the simulation was found to converge to the correct chemical potential distribution in 7 iterations ( $\beta_7 = 1.56 \times 10^{-4}$ ), requiring a total of approximately 100 hours CPU time on an AMD 2000+ processor. The form of  $\mu(\sigma)$  at the 1st, 3rd and 7th iterations are compared with the limiting equilibrium form in fig. 2. One sees that the principal effect of the reduction in  $\beta$  at each successive iteration is a decrease in the scatter of the solution; there seems to be no clear systematic dependence of the solution on the value of  $\beta$ . This feature was confirmed by independent runs at a number of other volume fractions and model parameters.

Fig. 3 shows a snapshot of a typical configuration obtained using the equilibrium solution for  $\mu(\sigma)$ . The configuration contains some  $1.1 \times 10^4$  particles. Although the form of  $\rho_t(\sigma)$  (fig. 1) dictates that the largest particles occur with a probability of less than 0.5% that of the average particle size, their far greater volume implies that they nevertheless occupy a sizeable fraction of the system volume. Herein lies the physical origin of the cross coupling between  $\bar{\rho}(\sigma)$  and  $\mu(\sigma)$ . Since the density (and

chemical potential) of the small particles depends on the available volume, it must therefore also depend on the density (and chemical potential) of the larger particles, and *vice-versa*.

Finally, for comparison, we have attempted to solve the same inverse problem using the equilibrium scheme of eq. 2. To initialize the chemical potential distribution, we took  $\mu_0(\sigma) = \ln(\rho_t(\sigma))$ . Some preliminary tuning of the damping factor  $\alpha$  and the run length of each iteration was found to be necessary in order for the method to converge. Trials with  $\alpha = 1.0$ ,  $\alpha = 0.5$  and  $\alpha = 0.25$  failed to converge in a reasonable timescale. For  $\alpha = 0.1$  the method did converge (in an oscillatory fashion), taking 93 iterations to reach the solution (compared to 7 iterations for the non-equilibrium method), and in so doing consuming some 230 hours of CPU time. A similar run, starting with  $\mu_0(\sigma) = 0 \forall \sigma$  (as used in the test of the non-equilibrium approach) did not converge, thus demonstrating the sensitivity of the method to the quality of the initial guess. For this particular problem, the non-equilibrium scheme is therefore computationally more efficient by at least a factor of two.

## V. DISCUSSION AND CONCLUSIONS

In this paper we have introduced a non-equilibrium iterative potential refinement scheme for inverse problems. As a test, the method was used to determine the chemical potential distribution for a LJ fluid having a wide distribution of particle sizes. We find it to be efficient, simple to implement and it requires no initial guess for the solution.

The efficacy of the new method arises from its application of continuous small modifications to  $\mu(\sigma)$  throughout the refinement, rather than large-scale updates between iterations as occurs in equilibrium schemes. The advantages of such an approach are apparent when one considers the high degree of cross coupling that can exist between  $\mu(\sigma)$  and  $\bar{\rho}(\sigma)$ , and the problem it implies: namely that a change to the chemical potential at any one value of  $\sigma$  can substantially affect the whole composition distribution. Accordingly it is desirable that (a) each individual modification to  $\mu(\sigma)$  is kept small in order to moderate the magnitude of cross coupling effects, and (b) such deviations from the target distribution that do arise are immediately corrected by further modifications to  $\mu(\sigma)$ . Our method achieves this by continually ‘tweaking’  $\mu(\sigma)$  by small amounts to iron out differences between the *instantaneous* form of  $\rho(\sigma)$  and the target.

With regard to convergence properties, our findings indicate that even for the earliest iterations, the method yields (at least for current problem) an estimate for  $\mu(\sigma)$  which, whilst statistically poor, does not appear to deviate systematically from the true solution. As iteration proceeds, it ‘hugs’ the solution ever more tightly, thereby allowing the degree of convergence to be judged solely on the basis of the statistical scatter of the solu-

tion. This remarkable feature would seem to promote reliable convergence to the true solution. One might additionally speculate that the intrinsically non-equilibrium character of the method generates “noise” that promotes escape from any local minima in the solution space, thus overcoming one of the apparent limitations of gradient-based refinement schemes.

The main factor that we have found to influence the reliability and rate of convergence in our method is the choice of the initial value of the modification factor  $\beta_0$  [27]. Should this value be chosen to be too large ( $\beta_0 > 0.05$ ) then the method may require an excessive number of iterations to converge, or in extreme cases (as also occurs in equilibrium schemes [14]), not converge at all. If, on the other hand, it is chosen very small ( $\beta_0 < 0.005$ ), then fewer iterations may be necessary overall, but the earlier iterations will take longer to complete because they require many more modifications steps. Within this window, the efficiency does not appear to vary by more than about a factor of 2, but there is certainly scope for trial and error optimization. We found that this is achievable quickly (during the initial stages of the first iteration) simply by monitoring the time evolution of  $\zeta$  (c.f. eq. 4). In cases where  $\beta_0$  is chosen too large for convergence, this quickly becomes evident during the first iteration because  $\zeta$  does not decrease steadily towards  $\zeta^*$ . This permits early diagnosis of convergence problems, in contrast to equilibrium schemes, where a

failure to converge is typically only apparent after a number of iterations.

Finally we note that although we have tested our method within the specific context of a polydisperse LJ fluid, its potential applicability is more wide ranging. As described in sec. I, a diverse range of inverse problems can be mapped onto a grand canonical polydisperse composition space [5]. It is simply a matter of identifying the analogue quantities to  $\rho(\sigma)$  and  $\mu(\sigma)$ ; thereafter the method can be applied exactly as we have described. Thus, for instance, in a molecular liquid, a (partial) structure factor  $g(r)$  might play the role of  $\rho(\sigma)$  while the interatomic pair potential  $\phi(r)$  plays the role of  $\mu(\sigma)$ . If applied to real experimental data in this way, it would be of interest to compare the robustness of our method with that of existing refinement schemes, particularly with regard to the sensitivity to experimental uncertainty in the target structural data and potential truncation effects [13].

### Acknowledgment

The author is grateful P. Sollich for discussions and to A.D. Bruce for a thought provoking murmur. This work was supported by the EPSRC, grant number GR/S59208/01 and the Royal Society.

- 
- [1] D. Levesque, J.J. Weis and L. Reatto, Phys. Rev. Lett. **54**, 451 (1985).
- [2] See eg. C. Hardacre, J.D. Holbrey, S.E.J. McMath, D.T. Bowron, A.K. Soper, J. Chem. Phys. **118**, 273 (2003).
- [3] See eg. M. Luzar, M.E. Rosen, S. Caldarelli, J. Phys. Chem. **100** 5098 (1996).
- [4] For a review see R.L. McGreevy, J. Phys. Condens. Matter **13**, R877 (2001).
- [5] G.C. Rutledge, Phys. Rev. **E63**, 021111 (2001).
- [6] L. Onsager, Ann. N.Y. Acad. Sci. **51**, 627 (1949).
- [7] An equivalent viewpoint (adopted in [5]) considers  $N$  pseudo particles speciated according to their position relative to the rest of the system. The species label is then formally an  $N$ -component vector  $\vec{\sigma}$  corresponding to the  $N$  interparticle distances. While this formulation obviates the need for a configurational constraint, the fact that  $\mu(\vec{\sigma})$  is defined on an  $N$ -dimensional space, renders it computationally cumbersome.
- [8] R.L. Henderson, Phys. Lett. **A49**, 197 (1974).
- [9] J. Zwicker and R. Lovett, J. Chem. Phys. **93**, 6752 (1990).
- [10] R.A. Evans, Mol. Simul. **4**, 409 (1990).
- [11] Here and throughout this paper, factors of the inverse temperature  $\beta$  have been absorbed into the effective chemical potential distribution.
- [12] J.-P. Hansen and I.R. MacDonald, *Theory of Simple Liquids*, Academic Press, London (1990).
- [13] A.K. Soper, Chem. Phys. **202**, 295 (1996).
- [14] A.P. Lyubartsev and A. Laaksonen, Phys. Rev. **E52**, 3730 (1995).
- [15] G. Tóth, J. Chem. Phys. **118**, 3949 (2003).
- [16] W.H. Press, S.A. Teukolsky, W.T. Vetterling, and B.P. Flannery, *Numerical Recipes in C: The Art of Scientific Computing*, 2nd ed., Cambridge Univ. Press, New York, (1992)
- [17] Although we have no definitive explanation for this observation, it seems likely that occasional iterations of the form Eq. 2 introduce noise into the minimization procedure, thereby enabling escape from local minima.
- [18] F.A. Escobedo, J. Chem. Phys. **115**, 5642 (2001); *ibid* 5653 (2001).
- [19] N.B. Wilding and P. Sollich, J. Chem. Phys. **116**, 7116 (2002).
- [20] A.M. Ferrenberg and R.H. Swendsen, Phys. Rev. Lett. **61**, 2635 (1988); *ibid* **63**, 1195 (1989).
- [21] A.K. Soper, Personal communication.
- [22] G. Tóth, J. Chem. Phys. **115**, 4770 (2001).
- [23] F. Wang and D.P. Landau, Phys. Rev. Lett. **86**, 2050 (2001). This method utilizes “on-the-fly” updating of a non-equilibrium estimate of the density of states of a system. MC acceptance probabilities are modified in such a way as to generate a flat histogram of states visited by a random walk in the energy.
- [24] *A priori*, one might expect faster convergence to result from an update of the form  $\mu'(\sigma) = \mu(\sigma) - \beta_i \ln(\rho(\sigma)/\rho_t(\sigma))$ . However in tests this was found not to be the case, presumably due to the smallness of the values of  $\beta_i$  employed. An advantage in employing the

update scheme Eq. 3 is that no numerical problems arise when  $\rho(\sigma) = 0$ .

- [25] Choosing  $2 \leq n \leq 5$  appears to yield an efficient scheme. Larger values reduce the number of iterations required to reach the limiting equilibrium form, but increase disproportionately the time required for each iteration to complete.
- [26] D. Frenkel and B. Smit; *Understanding Molecular Simulation*, Academic Press, Boston (1996).
- [27] In principle, convergence might also fail if one were to choose an excessively large value of  $\zeta^*$ . However, the value  $\zeta^* = 0.4$  we suggest here works well in all cases we have examined.

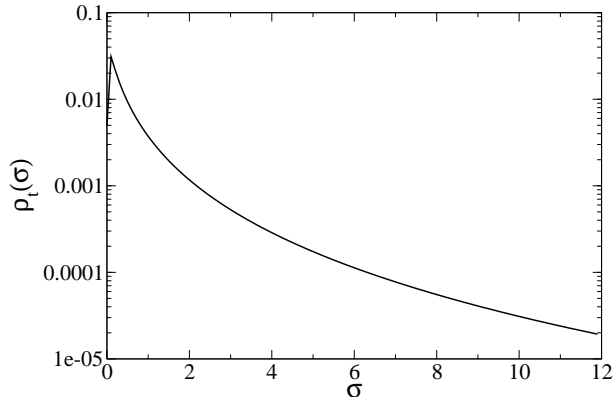


FIG. 1: The log-normal target distribution  $\rho_t(\sigma)$  described in the text and displayed on a logarithmic scale. The distribution has standard deviation  $W = 2.5$  and scale parameter  $\rho_t = 0.0152$ .

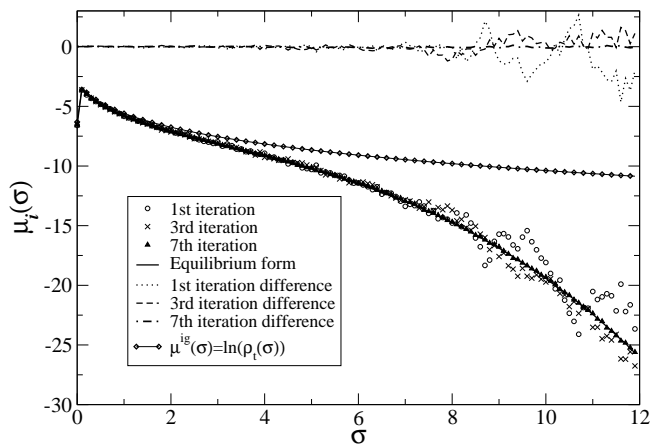


FIG. 2: The convergence of the non-equilibrium refine procedure. Shown (bottom part) are the forms of  $\mu_i(\sigma)$  at completion of iteration numbers 1, 3 and 7, together with the limiting equilibrium solution (solid line). Also shown for comparison is the potential of mean force  $\mu^{ig}(\sigma) = \ln(\rho_t(\sigma))$ . The upper part of the figure shows (on the same scale) a difference plot measuring the deviation from the final solution at each iteration.

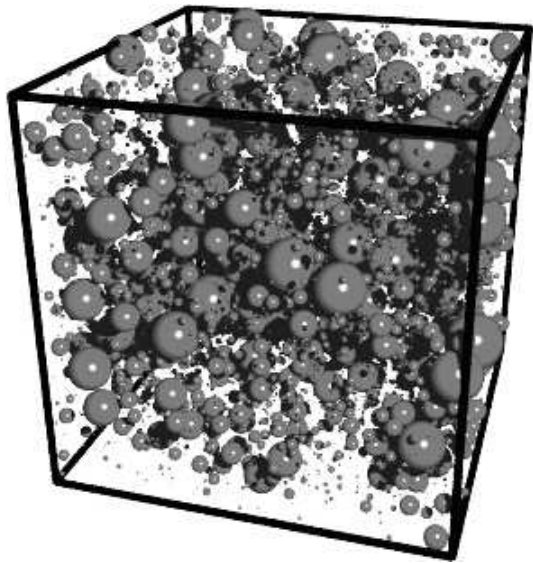


FIG. 3: Snapshot configuration of  $N = 11274$  polydisperse LJ particles drawn from the log-normal size distribution shown in fig. 1.

## APPENDIX A: GRAND CANONICAL FORMULATION OF POLYDISPERSITY

Here we provide a brief formal overview of the statistical mechanics of polydispersity. We consider a classical fluid of polydisperse particles confined to a volume  $V = L^d$ . The system is assumed to be thermodynamically open, so that the particle-number distribution  $N(\sigma)$  is a statistical quantity. The associated grand canonical partition function takes the form:

$$\mathcal{Z}_V = \sum_{N=0}^{\infty} \frac{1}{N!} \prod_{i=1}^N \left\{ \int_V d\vec{r}_i \int_0^{\infty} d\sigma_i \right\} \exp(-\beta \mathcal{H}_N(\{\vec{r}, \sigma\})) \quad (\text{A1})$$

with

$$\mathcal{H}_N(\{\vec{r}, \sigma\}) = \Phi(\{\vec{r}, \sigma\}) - \sum_{i=1}^N \mu(\sigma_i). \quad (\text{A2})$$

Here  $N$  is the overall particle number, while  $\beta = (k_B T)^{-1}$  and  $\mu(\sigma)$  are respectively the prescribed inverse temperature and chemical potential distribution.  $\{\vec{r}, \sigma\}$  denotes the *configuration*, i.e. the complete set  $(\vec{r}_1, \sigma_1), (\vec{r}_2, \sigma_2) \cdots (\vec{r}_N, \sigma_N)$  of particle position vectors and polydisperse attributes. The corresponding configurational energy  $\Phi(\{\vec{r}, \sigma\})$  is assumed to reside in a sum of pairwise interactions

$$\Phi(\{\vec{r}, \sigma\}) = \sum_{i < j=1}^N \phi(\vec{r}_i, \vec{r}_j, \sigma_i, \sigma_j), \quad (\text{A3})$$

where  $\phi$  is the pair potential.

The fluctuating particle number distribution is defined by

$$N(\sigma) \equiv \sum_{i=1}^N \delta(\sigma - \sigma_i), \quad (\text{A4})$$

with  $\sigma$  the continuous polydispersity attribute and  $N = \int N(\sigma) d\sigma$ . The associated composition distribution is

$$\rho(\sigma) \equiv N(\sigma)/V. \quad (\text{A5})$$

The statistical behavior of  $\rho(\sigma)$  is completely described by its probability distribution

$$p_V[\rho(\sigma)] = \frac{1}{Z_V} \sum_{N=0}^{\infty} \frac{1}{N!} \prod_{i=1}^N \left\{ \int_V d\vec{r}_i \int_0^{\infty} d\sigma_i \right\} \quad (\text{A6})$$

$$\times \exp(-\beta \mathcal{H}_N(\{\vec{r}, \sigma\})) \prod_{\sigma} \delta(\rho(\sigma) - N(\sigma)/V),$$

from which the ensemble averaged form of  $\rho(\sigma)$  follows as

$$\bar{\rho}(\sigma) = \int \rho(\sigma) p_V[\rho(\sigma)] d\rho(\sigma). \quad (\text{A7})$$